The Effect of Ligands on the Rates of the Metal Ion Promoted Decarboxylation of Oxaloacetate. A Model for the Active Site of an Enzyme?

N. V. Raghavan and Daniel L. Leussing*[1]

Contribution from the Department of Chemistry, The Ohio State University, Columbus, Ohio 43210. *Received August 9, 1976*

Abstract: Detailed investigations of the influence of glycine, alanine, histidine, glycylglycine, imidazole, and 1,10-phenanthroline on the Cu(II) catalyzed rates of decarboxylation and enolization of oxaloacetate have been performed. At amine concentrations comparable to those of the metal ion, large rate enhancements of decarboxylation are observed under certain conditions. Concurrently, enolization rates are inhibited. The effect of the amine is to surpress the formation of inactive dinuclear oxac complexes by reducing the metal ion activity in solution and to form mononuclear mixed ligand complexes. Except with phen, the $oxac^{2-}$ in these mixed ligand complexes appears to be in an environment similar to that found in the binary complex, Cu(oxac). The ternary complex, Cu(phen)oxac, undergoes decarboxylation and enolization at a faster rate than the other Cu(II)–$oxac^{2-}$ complexes, and also has a higher equilibrium enol content, owing to the effects of Π back-bonding. Coordinating groups likely to be found at the active site of an enzyme do not significantly influence coordinated $oxac^{2-}$. Calculations show that many of the differences observed between metal ion catalyzed enzymatic and nonenzymatic decarboxylation of $oxac^{2-}$ can be accounted for almost entirely by increases in the stabilities of the known complexes in the environment presented by the enzyme. The required stabilizations can be brought about in part by the presence of a low dielectric region at the enzyme active site.

It has been recognized for a number of years that various complexing agents produce diverse effects on the metal ion promoted rates of decarboxylation of oxaloacetate (oxac) and its derivatives. Steinberger and Westheimer[2] reported that the Cu(II) promoted rate of decarboxylation of α,α-dimethyl oxaloacetate is faster in pyridine buffers than in citrate or acetate buffers. Subsequent studies[3,4] have further shown that it is possible for 1,10-phenanthroline and its derivatives to enhance the activities of metal ions toward α,α-Me_2oxac. Munakata[5] and his co-workers in investigating the effects of many different kinds of ligands on the activities of Mn^{2+}, Co^{2+}, Ni^{2+}, Cu^{2+}, and Zn^{2+} toward $oxac^{2-}$ found that most ligands inhibited reaction rates but α,α'-bipyridyl (bdpy) and 1,10-phenanthroline (phen) enhanced the kinetic activities of all metal ions except those of Cu(II) where inhibition was observed. These authors report enhanced Cu(II) promoted rates only in the presence of histidine and its derivatives. In contrast, Yamane[6] et al. report that the presence of bpy, phen, or ethylenediamene (en) increases decarboxylation rates of Cu(II)–$oxac^{2-}$ mixtures. Bontchev and Michaylova[7] also found activation of Cu(oxac) decarboxylation by pyridine and picoline but none by methylamine and piperidine.

These ligand effects have been interpreted[2-8] as arising from electronic interactions in mixed ligand, Cu(L)oxac, complexes, where L represents a ligand other than a water molecule. Implications toward requirements at the metal ion binding site of metallodecarboxylases have been drawn from these observations;[2-5,7,8] however, it has been pointed out[2] that such conclusions must be regarded as tentative until the exact interactions in these model systems are known.

A recent detailed study[9] of the behavior of binary Cu(II)–$oxac^{2-}$ mixtures has demonstrated that the inhibition of decarboxylation, which occurs at higher pH and Cu(II) concentrations, arises from the formation of an inactive dinuclear enolate complex, $Cu_2(H_{-1}oxac)^+$. One effect of a second ligand will be to alter the distribution of $oxac^{2-}$ between the active mononuclear complex and the dinuclear complex, $Cu_2(H_{-1}oxac)^+ + L + H^+ \rightleftharpoons Cu(oxac) + CuL$. Another possible effect would be to induce changes in the enol content of the mononuclear complex by shifting the equilibrium

$$Cu(L)oxac_{keto} \overset{K_{enol}^{CuLox}}{\rightleftharpoons} Cu(L)oxac_{enol}$$

in one direction, or the other. It is the keto form that undergoes decarboxylation while the enol form is inactive.[2,10,11]

In this study we have endeavored to sort out these thermodynamic factors from the kinetic and to obtain the absolute values of the rate constants for the decarboxylation of the keto forms of the ternary mixed ligand complexes,

$$Cu(L)oxac_{keto} \xrightarrow{k_{-CO_2}^{CuLox}} CO_2 + \text{products}$$

It is only from a comparison of these values with the corresponding value obtained for the binary complex that legitimate conclusions can be drawn regarding the intrinsic influence of coordinated L on the decarboxylation of coordinated $oxac^{2-}$.

Experimental Section

Oxaloacetic acid, glycine, alanine, histidine, glycylglycine, and imidazole were obtained from Nutritional Biochemical Corp. 1,10-Phenanthroline was purchased from the G. Frederick Smith Chemical Co. Stock solutions of these reagents were prepared by weight, those of oxac being freshly prepared prior to use. Analysis of the oxac by titration with standardized NaOH indicated a purity of 97.7%. Copper(II) chloride stock solutions were prepared from J. T. Baker Chemical reagent grade material and analyzed by the method of Schwarzenbach and Flaska.[12]

Kinetic determinations were initiated by mixing two solutions, one containing Cu(II) and amine, the other oxac. Low levels of acetic acid and sodium acetate were present in both solutions to help maintain the pH constant at the desired value. Variations in pH were made by adding NaOH or HCl solutions to the Cu(II) solutions. The actual pH was measured at the end of a reaction using a Radiometer Model 25 pH meter.

In order to obviate complications arising from the formation of $Cu(oxac)_2^{2-}$ either an excess of Cu^{2+} over $oxac^{2-}$ or very dilute solutions were employed. Rate determinations employing the reverse order, $oxac^{2-} > Cu(II)$, may be complicated by a change in the distribution of the solution species from one containing appreciable quantities of $Cu(oxac)_2^{2-}$ in the beginning of the reaction to one in which this species is almost totally absence as $oxac^{2-}$ disappears.

Most kinetic experiments were run at 0.0025 M Cu(II), 1×10^{-4} M oxac. Variations in Cu(II) concentration were made, however, to better define the influence of polynuclear species. The range of amine concentrations and pH range employed for a given amine were determined in part from a consideration of the Cu(II)–amine stability constants. It is most desirable to run reactions under conditions where

Scheme I

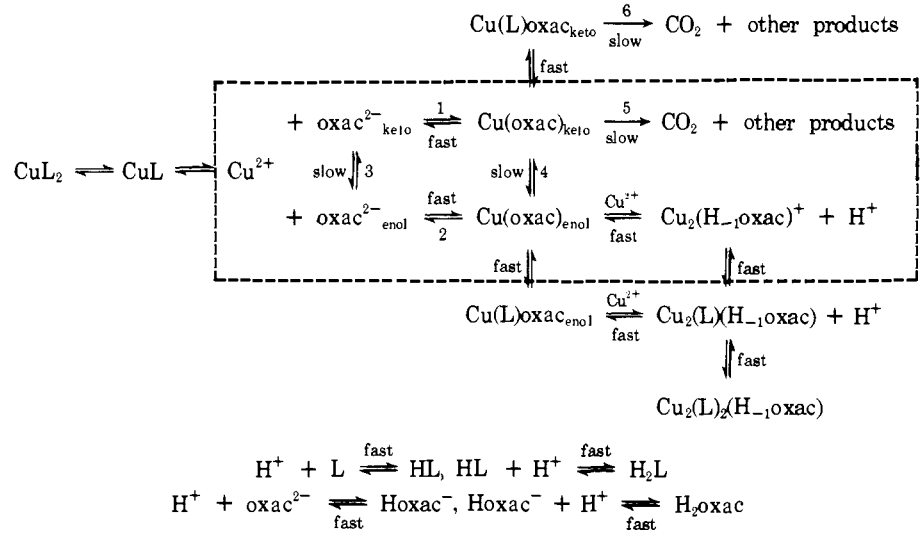

$$H^+ + L \underset{\text{fast}}{\rightleftharpoons} HL,\ HL + H^+ \underset{\text{fast}}{\rightleftharpoons} H_2L$$

$$H^+ + oxac^{2-} \underset{\text{fast}}{\rightleftharpoons} Hoxac^-,\ Hoxac^- + H^+ \underset{\text{fast}}{\rightleftharpoons} H_2oxac$$

1:1 Cu(II):amine complexes prevail (not necessarily where the ratios of the total concentrations are unity). With the exception of phen and his, which form very stable complexes with Cu(II), the amine concentrations lay in the range 0.004–0.03 M, with the pH being varied from 3.8 to 6.0. A total of 29, 27, 18, and 20 data points were determined, respectively, for the gly, ala, glygly, and im systems. With his a concentration range of 0.001–0.02 M was used at pH 3.2–5.2, 46 data points, while the phen concentrations were 0.00057–0.0016 M at pH 3.1–4.1, 23 data points. The ionic strength of all solutions was adjusted to 0.1 by the addition of KCl. All experiments were run at 25 °C.

A Durrum-Gibson stopped flow spectrophotometer was used to measure the enolization rates, which are complete in about 20–30 s. Slower decarboxylation was followed spectrophotometrically using a Cary 14 spectrophotometer. Wavelengths of 290–300 nm were employed. Pressure changes arising from release of CO_2 were followed in some experiments. A Texas Instruments Precision Pressure Gauge Model 145-01 was used, the output being recorded on a strip chart recorder. Experiments were performed using reaction solutions containing 0.015 M Cu(II), 0.015 M amine, and 0.006 M oxac at either pH 3.5 (1,10-phen, his), or 4.0 (gly^-). Biphasic pressure changes were noted in the presence of all of these ligands.

Nonlinear least-squares curve fitting analyses were performed using a computer program developed in our laboratories, CORNEK II. This program is similar to the original version which was developed to fit rate constants to labile complex ion systems,[13] but has been modified to fit equilibrium constants, also. The present data were treated in essentially the same manner as those obtained previously.[9] The inclusion of the binary and ternary complexes into the analysis was easily accomplished owing to the generality of the computer program.

Analysis of the Data

The interactions which occur in Cu(II)-$oxac^{2-}$ solutions in the absence of a second ligand, L, are depicted in Scheme I within the portion enclosed by the dashed lines.

Initially, $oxac^{2-}$ is present to greater than 90% in the keto form. When Cu(II) is added, complexation and proton redistribution reactions occur very rapidly. Following this initial stage three distinct and slower reactions are observable: enolization (paths 3 and 4) and fast decarboxylation (path 5) which together make up a single relaxation, τ_1, requiring about 20–30 s; protonation of the Cu(II) pyruvate enolate that is the immediate reaction product of 5; and, slow decarboxylation, τ_3, over a period of 10–30 min.[9] The process giving rise to τ_2 is manifested through pH changes and was not followed in this study. τ_3 arises from the decarboxylation along 5 of the low steady state or quasi-equilibrium concentration of $Cu(oxac)_{keto}$ that remains after the τ_1 phase. As this complex decarboxylates, its concentration is replenished by the reketonization of $Cu(oxac)_{enol}$.

The effective pseudo-first-order rate constant for the slow decarboxylation of Cu(oxac) ($1/\tau_3$) is related to the true rate constant by the relationship,

$$1/\tau_3 = f_{Cu(oxac)_{keto}} k_{-CO_2}^{Cu(ox)} \qquad (1)$$

where $f_{Cu(oxac)_{keto}}$ is the fraction of total $oxac^{2-}$ present in the form of the keto complex. In a ternary complex, either one, or both, of $f_{CuLoxac_{keto}}$ and $k_{-CO_2}^{CuLox}$ may differ from that of the binary complex.

When the rate constants for the enolization/ketonization reaction are sufficiently faster than that for decarboxylation, as is the situation with many metal ions and is close to that with Cu(II), then a preequilibrium condition essentially exists and eq 1 takes the form,

$$1/\tau_3 = \frac{1}{1 + K_{enol}^{Moxac}} f_{Moxac} k_{-CO_2}^{Moxac} \qquad (2)$$

where f_{Moxac} is equal to the fraction of oxac bound as Moxac (both keto and enol forms). The value of f_{Moxac} is obtained using the macroscopic equilibrium constants which encompass both keto and enol forms.

As a reasonably good first approximation eq 2 can be applied to the Cu(II) mediated reactions; however, following the earlier treatment,[9] exact relationships describing the near equilibrium kinetics (NEK) of two coupled reactions were employed here. The NEK equations are identical with the earlier ones, except for suitable modifications described below to take into account the presence of L.

The addition of L to Cu(II)-$oxac^{2-}$ solution will bring about the formation of binary Cu(II)-L and ternary Cu(II)-L-$oxac^{2-}$ complexes. The additional species and reaction paths expected are shown in the expanded part of Scheme I. Because the reactions of L with the various Cu(II) species and H^+ are fast, the presence of L does not change the number of rate equations which characterize the rate processes of interest. Only two independent rate equations can be written. Choosing these to describe the rate of CO_2 loss and the rate of enol formation yields the following,

$$\frac{dCO_2}{dt} = k_{-CO_2}^{Cu(oxac)}[Cu(oxac)] + k_{-CO_2}^{CuLoxac}[Cu(L)oxac] + k_{-CO_2}^{Hoxac}[Hoxac^-] + k_{-CO_2}^{oxac}[oxac^{2-}] \qquad (3)$$

$$\frac{d[oxac_{enol}]_\Sigma}{dt} = k_1[H^+][Hoxac_{keto}] + k_2[H^+][oxac_{keto}^{2-}] + k_3[HOAc][oxac_{keto}^{2-}] + k_4[H^+][Cu(oxac)_{keto}] + k_5[Cu(oxac)_{keto}] + k_6[H^+][Cu(L)oxac_{keto}] + k_7[Cu(L)oxac_{keto}] - k_{-1}[H^+][Hoxac_{enol}] - \ldots + \text{analogous terms involving [HL] and [L] catalysis} \qquad (4)$$

Table I. Equilibrium Constants for Cu(II)-oxac^{2-}-Ligand Ternary Systems: 25 °C, I = 0.10

Ligand	Log overall formation constant							K_{enol}[b]
	HL,[a] M^{-1}	H_2L,[a] M^{-2}	CuL,[a] M^{-2}	CuL_2,[a] M^{-2}	Cu(L)oxac, M^{-2}	$Cu_2(L)(H_{-1}oxac)$, M^{-2}	$Cu_2(L)_2(H_{-1}oxac)$, M^{-3}	
H_2O	—	—	—	—	4.15	2.55 (ref 9)	—	12 (fit)
Glycine	9.68	12.01	8.27	15.19	12.02 (fit)	10.42 (est)	17.6 (fit)	11 (fit)
Alanine	9.59	12.12	8.22	15.07	11.87 (est)	10.27 (est)	17.2 (fit)	12 (fit)
Histidine[c]	9.08	15.06	10.21	18.53	14.48 (fit)	12.88 (fit)	21.8 (fit)	11 (fit)
Glycylglycine[d]	8.0	11.06	5.43	8.64	Negligible	Negligible	Negligible	—
Imidazole	7.09	—	4.26	7.87	Negligible	Negligible	Negligible	—
1,10-phenanthroline	4.96	—	8.82	15.39	13.42 (fit)	11.82 (fit)	20.0 (fit)	30 (fit)

[a] Reference 29. [b] $Cu(L)oxac_{keto} \rightleftarrows Cu(L)oxac_{enol}$. [c] In addition the following species were included (log β): (Hhis)Cu(oxac) (18.41) (fit, assuming the pK_a is the same as that of Cu(his)H^{2+} (14.13), Cu(his)$_2H^+$ (23.65), Cu(his)$_2H_2^{2+}$ (26.85). It was also assumed that $k_{-CO_2}^{Cu(Hhis)oxac} = k_{-CO_2}^{Cu(his)oxac}$. [d] Cu(glygly)$_2H_{-1}^-$, log β = 4.57; Cu(glygly)H_{-1}, log β = 1.43.

where,

$$[oxac_{enol}]_\Sigma = [H_2oxac_{enol}] + [Hoac_{enol}^-] + [oxac_{enol}^{2-}] + [Cu(oxac)_{enol}] + [Cu(L)oxac_{enol}] + [Cu_2(H_{-1}oxac)^+] + [Cu_2(L)(H_{-1}oxac)] + [Cu_2(L)_2(H_{-1}oxac)] \quad (5)$$

Owing to the pseudo-first-order condltions used, in which all components were present in excess of oxac, it is convenient to express the concentrations of the oxac species in fractional form,

$$\frac{d(CO_2)}{dt} = (k_{-CO_2}^{Cu(oxac)} f_{Cu(oxac),keto} + k_{-CO_2}^{CuLoxac} f_{CuLoxac,keto} + k_{-CO_2}^{Hoxac} f_{Hoxac,keto} + k_{-CO_2}^{oxac} f_{oxac,keto})[oxac_{keto}]_\Sigma \quad (6)$$

$$\frac{d[oxac_{enol}]_\Sigma}{dt} = (k_1[H^+]f_{Hoxac,keto} + \ldots + k_4[H^+]f_{Cu(oxac),keto} + \ldots)[oxac_{keto}]_\Sigma - (k_{-1}[H^+]f_{oxac,enol} + \ldots)[oxac_{enol}]_\Sigma + \text{catalytic [HL] and [L] terms} \quad (7)$$

$[oxac_{keto}]_\Sigma$ represents the total amount of oxac in the keto form. The values of $[oxac_{enol}]_\Sigma$, $[oxac_{keto}]_\Sigma$, and the fractions are calculated for the steady state condition that exists after the completion of the τ_1 phase. This is the region for which the macroequilibrium constants have been determined.

The fractional distribution of oxac is calculated by first solving the three macroscopic mass balance and 8 + N equilibrium equations which apply to a given set of experimental conditions. The mass balance equations are,

$$Cu_\Sigma = [Cu^{2+}] + [CuL] + [CuL_2] + [Cu(oxac)] + [Cu(L)oxac] + 2[Cu_2(H_{-1}oxac)^+] + 2[Cu_2(L)(H_{-1}oxac)] + 2[Cu_2(L)_2(H_{-1}oxac)] \quad (8)$$

$$oxac_\Sigma = [H_2oxac] + [Hoxac^-] + [oxac^{2-}] + [Cu(oxac)] + [Cu_2(H_{-1}oxac)^+] [Cu(L)oxac] + [Cu_2(L)(H_{-1}oxac)] + [Cu_2(L)_2(H_{-1}oxac)] \quad (9)$$

$$L_\Sigma = \sum_i^N [H_iL] + [L] + [CuL] + 2[CuL_2] + [Cu(L)oxac] + [Cu_2(L)(H_{-1}oxac)] + 2[Cu_2(L)_2(H_{-1}oxac)] \quad (10)$$

The constants for the formation of the binary species are readily available from the literature. The values used in this study are given in Table I. The formation constants of the mixed ligand complexes are not known initially, but values were estimated using approaches outlined by Sigel.[16,17] Attempts to improve these values by fitting them to the data were made using CORNEK II. With a given set of constants and specified total concentrations it is possible to solve the set of equations for the equilibrium concentrations of the macroscopic species. The microscopic concentrations of the keto and enol isomers of the various forms of oxac^{2-} were then obtained using expressions of the type,

$$[Xoxac_{enol}] = [Xoxac] \frac{K_{enol}^{Xoxac}}{1 + K_{enol}^{Xoxac}} \quad (11)$$

and

$$[Xoxac_{keto}] = [Xoxac] \frac{1}{1 + K_{enol}^{Xoxac}} \quad (12)$$

where K_{enol}^{Xoxac} is the equilibrium constant for the general reaction, $Xoxac_{keto} \rightleftarrows Xoxac_{enol}$ and [Xoxac] is the macroscopic concentration. Values of $K_{enol}^{CuLoxac}$ are not known initially and these, too, must be estimated, and refined whenever possible.

The fractional distribution of oxac^{2-} is then obtained, and the results substituted into the NEK equations derived from eq 6 and 7.[9] However, before the iterative curve-fitting procedure could be begun initial guesses of the rate constants for the reactions of the mixed ligand complexes had to be provided. These were then fit to the data. The starting values were usually taken to be the same as those for the analogous reactions of the binary Cu(II)-oxac^{2-} species, but in successive runs these initial values were often varied to determine the effect on the final result and conclusions.

In no case, were the constants which we report here obtained from a single computation. Various models were tested using different values of mixed ligand equilibrium and rate constants. Reaction paths and complexes were made dominant, or omitted entirely. Sometimes the inclusion of a given path or complex was found to improve the fit slightly, but the uncertainty in the associated parameter was shown to be comparable to, or larger than, the value obtained. This was taken to mean that the experimental data did not define this species, or reaction, sufficiently well to warrant its inclusion in further computations. Fortunately, it was found that the inclusion, or omission, of such paths had little influence on the values determined for the dominant reactions. It was also found that the best results were obtained by treating the τ_1 and τ_3 data simultaneously. The concentration-rate profiles for both sets of these data are determined by the same macroscopic formation constants. This redundancy hastens the convergence of the computations to the best fit.

Results

At the lower concentration levels examined, the addition of each of the amines investigated was found to cause an increase

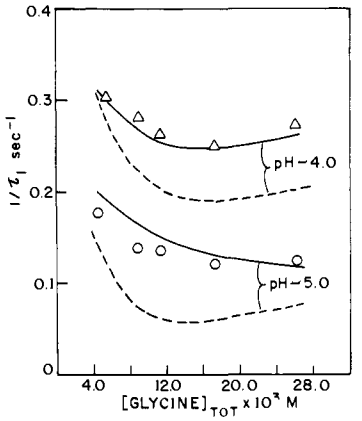

Figure 1. The influence of glycine on the experimental first-order rate constant for the first set of rate processes (0.0025 M Cu(II), 1×10^{-4} M $oxac_{tot}$): - - -, calculated for the simple model; —, calculated including mixed ligand complexes. Enolization is the primary reaction, but fast decarboxylation also contributes to the rate.

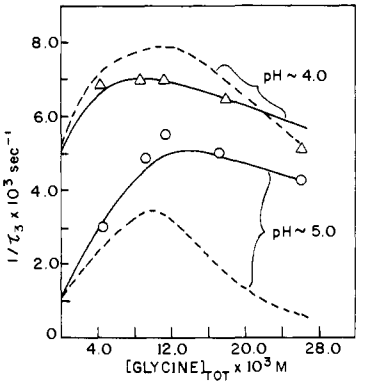

Figure 2. The influence of glycine on the experimental first-order rate constant for slow decarboylation (0.0025 M Cu(II), 1×10^{-4} M $oxac_{tot}$): - - -, calculated for the simple model; —, calculated including mixed ligand complexes.

in τ_3, the rate of slow decarboxylation, and a decrease in τ_1, largely enolization. At the higher amine concentrations, the effects were reversed with decarboxylation inhibited and enolization activated. These effects can be seen in the rate-amine concentration profiles for data obtained at pH 4.0 (triangles) and pH 5.0 (circles) in Figures 1-4. The intercepts along the vertical axes of these figures indicate the rates at zero amine concentration. The marked influence of amine is apparent by comparing the observed trends with these intercepts.

To determine the extent to which the observed effects arise solely from the formation of CuL and CuL_2, thereby altering the relative amounts of Cu(oxac) and $Cu_2(H_{-1}oxac)^+$ in the reaction systems, computations were made neglecting the formation and reactivities of any mixed ligand complexes. In these calculations all of the stability and rate constants necessary to calculate theoretical rates were known initially. The results for τ_1 and τ_3 based on this simple model are shown plotted as the dashed lines in Figures 1-5. The calculated changes in $oxac^{2-}$ distribution accompanying the addition of gly^- as a typical ligand at pH 5.0 are shown in panels A, B, and C of Figure 6.

It is readily seen in these curves that the addition of gly^- to the Cu(II)-$oxac^{2-}$ solution does indeed bring about a marked decrease in the fraction of $oxac^{2-}$ present as $Cu_2(H_{-1}oxac)^+$ with corresponding increases in the proportions of Cu(oxac) and free $oxac^{2-}$. The Cu(oxac) concentration reaches a maximum at about 10 mM gly^-. The rate of slow decarboxylation

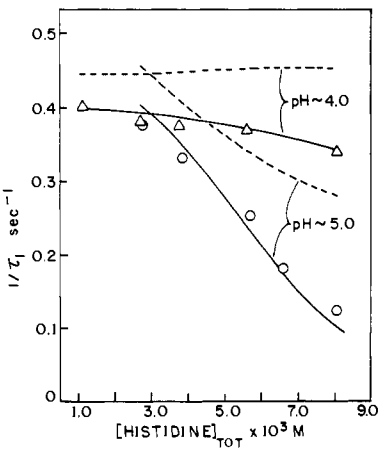

Figure 3. The influence of histidine on the experimental first-order rate constant for the first set of rate processes (0.0025 M Cu(II), 1×10^{-4} M $oxac_{tot}$): - - -, calculated for the simple model; —, calculated including mixed ligand complexes.

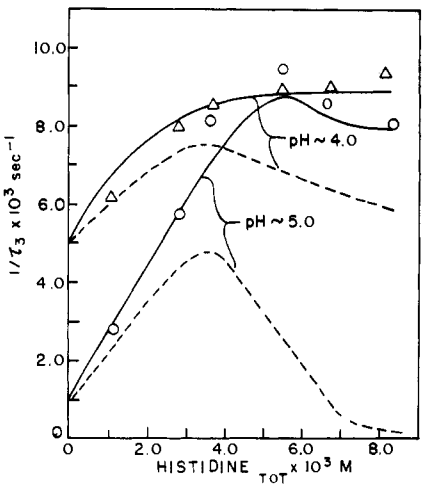

Figure 4. The influence of histidine on the experimental first-order rate constant for slow decarboxylation (0.0025 M Cu(II), 1×10^{-4} M $oxac_{tot}$): - - -, calculated for the simple model; —, calculated including mixed ligand complexes.

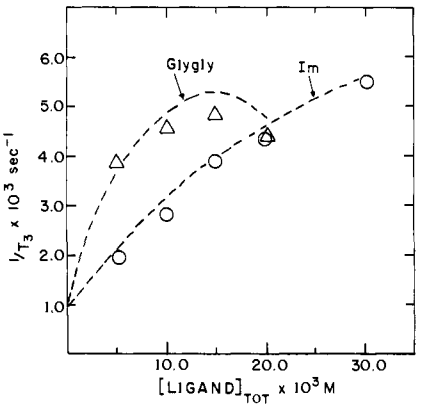

Figure 5. The influence of glycylglycine and imidazole on the experimental first-order rate constant for slow decarboxylation (0.0025 M Cu(II), 1×10^{-4} M $oxac_{tot}$, pH 5.0): - - -, calculated for the simple model.

increases as Cu(oxac) increases, but because proton catalyzed rates of enolization are faster for uncomplexed $oxac^{2-}$ enolization rates become slower. Above 10 mM, gly^- competes more successfully with $oxac^{2-}$ for Cu(II) and extensive amounts of free $oxac^{2-}$ are liberated. Decarboxylation rates

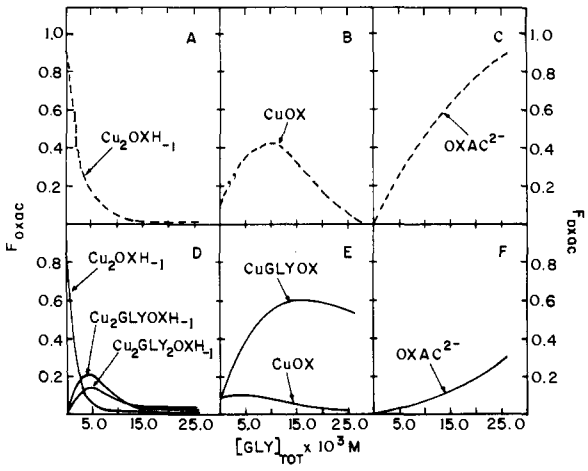

Figure 6. The influence of glycine on the distribution of oxac (0.0025 M Cu(II), 1×10^{-4} M $oxac_{tot}$): - - -, calculated for the simple model; —, calculated including mixed ligand complexes.

decrease and those for enolization increase. Theoretically rates calculated on the basis of this species distribution are shown as the dashed lines in Figures 1 and 2. Generally, poor agreement with the observed data points for both enolization and decarboxylation processes is obtained, although, qualitatively, the calculated curves exhibit some of the trends which are observed. Similar discrepences were also obtained between observed and calculated rates for the influence of alanine, histidine (Figures 3 and 4), and 1,10-phenanthroline on the Cu(II)-oxac reactions. Only with imidazole and glycylglycine was this simple model found to adequately account for the observations (Figure 5). In the case of the other ligands it was found necessary to include the formation and reactivity of the mixed ligand complexes which are shown in Scheme I, as well as, the binary complexes.

Owing to the large number of unknown equilibrium and rate constants introduced by the inclusion of the mixed ligand complexes it was felt not feasible to try to evaluate all the parameters which would appear in general rate equations written for these systems. From a consideration of the earlier results, several simplifying assumptions seemed warranted. In particular, most of the large number of catalytic paths potentially available for enolization do not appear to be important.

It had been found earlier that proton catalyzed paths for the enolization of $Cu(oxac)_{keto}$ are important at low pH, but the uncatalyzed (or H_2O catalyzed) paths becomes dominant above pH 3. Similarly, the low levels of acetate buffer employed in these studies permitted HOAc and OAc^- catalyzed pathways to be neglected. Thus, under the conditions where mixed ligand complexes are formed (pH >3) the dominant path for the enolization of the mixed ligand complex was assumed to be the uncatalyzed path,

$$Cu(L)oxac_{keto} \underset{k^{L}_{keto}}{\overset{k^{L}_{enol}}{\rightleftharpoons}} Cu(L)oxac_{enol}$$

The inclusion of only this path in the rate expression for path 4 was found to account reasonably well for the observed rates. However, at the higher amine concentrations used, deviations occurred which were suggestive of catalysis by the protonated forms of the amines. These contributions were not sufficiently important to permit them either to be resolved into the component terms or even to be accurately evaluated, so a single rate constant was assumed to apply to the catalyzed enolization of both the aquo and mixed ligand complexes,

$$Cu(oxac)_{keto} + HL \underset{k^{HL}_{keto}}{\overset{k^{HL}_{enol}}{\rightleftharpoons}} Cu(oxac)_{enol} + HL$$

and,

$$Cu(L)oxac_{keto} + HL \underset{k^{HL}_{keto}}{\overset{k^{HL}_{enol}}{\rightleftharpoons}} Cu(L)oxac_{enol} + HL$$

Values of k^{HL}_{enol} were found to fall in the range of 5-10 M^{-1} s^{-1} over all of the amines investigated, except with phen where this type of catalysis was not observed. This last result arises, at least in part, to the lower ligand concentrations employed with phen and does not necessarily imply that neither $Hphen^+$ nor phen are inactive in this respect.

The results of measurements of the pressure changes from CO_2 evolution in the ternary mixtures also permitted a reduction in the number of parameters to be evaluated. These pressure changes were found to be biphasic just as was observed in the binary Cu(II)-oxac mixtures.[9] The biphasic pressure change is observed when the absolute rate of decarboxylation along path 5 is approximately the same as that for enolization along paths 3 and 4. When Cu(II) and $oxac^{2-}{}_{keto}$ are mixed, $oxac^{2-}{}_{keto}$ disappears along all of these paths, giving rise to a burst of CO_2 as well as to enol formation during the τ_1 stage.

The volume of CO_2 released in the τ_1 stage was found to correspond to 20 ± 2% of the total volume evolved by the end of the reaction when all of the oxac had undergone decarboxylation, regardless of the presence of glycine, histidine, or 1,10-phenanthroline. This is the same percentage as was found for Cu(oxac) alone[9] and shows that the ratios of the initial fast rates of decarboxylation to enolization of $Cu(L)oxac_{keto}$ are fairly independent of L. Accordingly, for the mixed complexes the ratios of the rate constants $k_{-CO_2}{}^{CuLoxac}/k_{enol}{}^{CuLoxac}$ were assumed to have the same value as was found for $Cu(oxac)_{keto}$, 0.46, permitting $k_{-CO_2}{}^{CuLoxac}$ to be expressed as a function of $k^{L}{}_{enol}$. Thus, with these simplifications and estimates of the mixed ligand complex formation constants attempts were made in the preliminary calculations to fit only the three parameters, $k^{L}{}_{enol}$, $k^{HL}{}_{enol}$, and $K_{enol}{}^{CuLoxac}$, to the rate data.

The initial trials indicated the existence of a major inconsistency between the observed results and the assumed reaction model. This appeared to have its origins in the formation constants chosen for the bis dinuclear complexes, $Cu_2(L)_2(H_{-1}oxac)$. The values as estimated according to Sigel[16,17] appeared to be too high, and molecular models showed that two coordinated L molecules can sterically interfere with each other. Therefore, in subsequent computations best least-squares values of the formation constants of the $Cu_2(L_2)(H_{-1}oxac)$ complexes were also obtained, giving up to four parameters to be determined for each ternary system. By fitting the results for both the slow and fast processes simultaneously, ample data points were available to yield good values for all the constants determined. Indeed, in the experiments with phen and his the data were sufficiently sensitive to the concentrations of the Cu(L)oxac complexes that it was found possible to obtain least-squares values of their formation constants. The calculated values were found to agree with the estimated values within the uncertainties in the latter. The results of all these calculations are given in Tables I and II and the theoretical rate curves obtained using them are shown plotted as the solid curves in Figures 1-5. Good agreement between observed and calculated values is seen to have been obtained. The calculated distribution of $oxac^{2-}$ when mixed complexes are formed is shown in panels D, E, and F of Figure 6. The most important change is the conversion of $oxac^{2-}$ to $Cu(gly)oxac^-$.

Discussion

Figures 1-5 show that the presence of a second ligand, L, has a marked effect on the velocities of both the fast and slow processes. Glycylglycine, which is a tridentate ligand, and imidazole, which forms weak monodentately bound complexes with Cu(II), do not form significant concentrations of mixed

Table II. Rate Constants for the Enolization and Decarboxylation of Cu(L)oxac: 25 °C, $I = 0.10$

	A. Enolization Rate Constants k_{enol},[a] $M^{-1}\ s^{-1}$ or s^{-1}	Ref
$oxac^{2-}_{keto} + H^+$	1.4×10^3	9
$oxac^{2-}_{keto} + HOAc$	5.7	9
$Hoxac^-_{keto} + H^+$	7.5	9
$Cu(oxac)_{keto}$	0.37	9
$Cu(oxac)_{keto} + H^+$	280	9
$Cu(gly)oxac^-_{keto} \rightarrow Cu(gly)oxac_{enol}$	0.2	This work
$Cu(ala)oxac^-_{keto} \rightarrow Cu(ala)oxac_{enol}$	0.2	This work
$Cu(his)oxac^-_{keto} \rightarrow Cu(his)oxac_{enol}$	0.35	This work, $k_{enol}^{his} = k_{enol}^{Hhis}$
$Cu(phen)oxac_{keto} \rightarrow Cu(phen)oxac_{enol}$	0.83	This work
	B. Decarboxylation Rate Constants[a] $10^3 k_{-CO_2}$ (s^{-1})[a]	Ref
$oxac^{2-}$	0.017	11
Hoxac	0.057	11
H_2oxac	0.0011	11
$Cu(oxac)_{keto}$	170	9
$Cu(gly)oxac_{keto}$	100	This work
$Cu(ala)oxac_{keto}$	100	This work
$Cu(his)oxac_{keto}$	160	This work, $k_{-CO_2}^{Cu(his)oxac} = k_{-CO_2}^{CuHhis(oxac)}$
$Cu(phen)oxac_{keto}$	380	This work

[a] The values obtained in this work are least-squares results.

ligand Cu(II)-$oxac^{2-}$ complexes under the conditions employed in this study. Nevertheless, even these ligands were found to enhance the rates of decarboxylation by factors of 4-5-fold (Figure 5). Enolization rates are decreased, but by smaller factors. The ligand effect in these cases is indirect and is entirely attributable to the suppression of the formation of inactive dinuclear enolate complexes. These results dramatically demonstrate that large changes in rate can be produced which do not have their origins in electronic effects transferred from one ligand to another via a metal ion in a mixed ligand complex. Since this type of behavior is expected for any ligand, in general, corrections for these thermodynamic effects must be made before it is safe to draw conclusions regarding the kinetic behavior of the mixed ligand complex. The results for glycylglycine (Figure 5) also show the inhibition of decarboxylation which arises from the displacement of $oxac^{2-}$ from the Cu(II) coordination sphere as the Cu(II)-glygly$^-$ complexes are formed in increasing amounts. This effect of excess ligand is, also, expected to be general.

When glycine, alanine, histidine, or phenanthroline was added to Cu(II)-$oxac^{2-}$ solutions, additional rate effects atrributable to the formation of mixed ligand complexes were observed. The presence of these complexes has a marked influence on the distribution of $oxac^{2-}$ as shown by the solid lines in Figure 6. In this case the addition of glycine to the reaction mixture is seen to convert a solution in which 90% of the $oxac^{2-}$ is initially bound as inactive $Cu_2(H_{-1}oxac)^+$ to one in which relatively high concentrations of active Cu(gly)$oxac^-$ are formed. Large excesses of glycine still cause free $oxac^{2-}$ to be liberated, but higher concentrations of gly$^-$ are required than in the case where ternary complexes are not formed. Even though $Cu_2(H_{-1}oxac)^+$ has been assumed to bind gly$^-$ with the same affinity as Cu(oxac), it is seen that $Cu_2(gly)(H_{-1}oxac)$ is not a major component. The observed low stability of the higher gly$^-$ dinuclear complex, $Cu_2(gly)_2(H_{-1}oxac)^-$, further aids the conversion of inactive dinuclear to active mononuclear species.[18] Ala, his, and phen give similar behavior. While minor quantitive differences were found to exist in the distribution curves for these other ligands, the general shapes are the same as those shown in Figure 6.

With ternary complexes containing glycine, alanine, or histidine the ratios of $Cu(L)oxac_{enol}/Cu(L)oxac_{keto}$ were found to be identical, within the accuracy of the measurements, to that of Cu(oxac), itself (see Table I). This is not a surprising result since as large a change as substituting Zn(II) for Cu(II) causes a change of only a factor of 2 in the $Moxac_{enol}/Moxac_{keto}$ ratio. On the other hand, 1,10-phenanthroline coordination yields a mixed complex having a significantly higher enol content than Cu(oxac). Increased rates of decarboxylation of Me_2oxac^{2-} [3] and high mixed ligand complex formation constants in the presence of phen[16] have been attributed to Π back-bonding. The increase in enol content appears to be another manifestation of this effect.

The forward rate constant for the uncatalyzed reaction,

$$Cu(L)oxac_{keto} \xrightarrow{k^{L}_{enol}} Cu(L)oxac_{enol}$$

was found to be the same as that of $Cu(oxac)_{keto}$ when L is histidine, but slightly smaller values were found for glycine and alanine. The last values are known with less accuracy, so not much significance should be attached to the quantitative differences observed between the values shown in Table I for these three ligands. Although, these values are somewhat similar, $Cu(phen)_{keto}$ once again shows deviating behavior with a significantly higher rate constant for enolization.

The independence on L of the ratio of $Cu(L)oxac_{keto}$ which decarboxylates to that which enolizes on first forming the complexes demonstrates that the rate constants for these two processes lie in a fixed proportion to one another. Therefore, the trends noted above for enolization pathways are paralleled in the rate constants for CO_2 loss. Gly, ala, or his coordination yields values that are comparable to that for the decarboxylation of $Cu(oxac)_{keto}$, but a higher value is found with 1,10-phenanthroline coordination. While the last result is in agreement with earlier observations concerning the effect of phen on the decarboxylation rates of α,α-Me_2oxac^{2-},[3,4] it should be noted that, because phen coordination increases K_{enol}, the net increase in CO_2 loss observed with oxac is less than expected solely on the increase in the value of $k_{-CO_2}^{Cu(phen)oxac}$. Equation 2 shows when $K_{enol}^{CuLoxac} > 1$, as is the case for Cu(II), increases in both $k_{-CO_2}^{CuLoxac}$ and

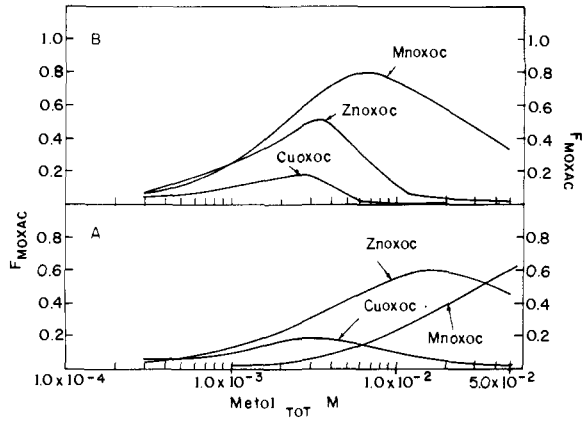

Figure 7. The influence of Mn(II), Cu(II), and Zn(II) concentrations on the fraction of oxac present as the active complex (0.0037 M $oxac_{tot}$, pH 5.0): panel A, curves calculated using the experimentally determined formation constants of Moxac and $M_2(H_{-1}oxac)^+$; panel B, curves calculated assuming enhanced complex stabilities (see text).

$K_{enol}^{CuLoxac}$ will tend to cancel. It follows that this effect will be less for metal ions having $K_{enol} < 1$.

It is now possible to understand the apparently contradictory results reported by Yamane[6] and Munakata[5] concerning ligand effects on slow decarboxylation rates. In the former study, sufficiently high Cu(II) concentrations were employed that appreciable quantities of the inactive dinuclear complexes were formed. Thus, the addtion of any coordinating ligand, even ethylenediamine, should cause an increase in the rate of the slow CO_2 evolution process. In the latter study, very low metal ion concentrations were used, together with a large excess of $oxac^{2-}$ over metal ion. Under these conditions, concentrations of the dinuclear complex are calculated to be negligible, and, in addition, Cu(II) is likely to be bound as the bis complex, $Cu(oxac)_2^{2-}$.[19] Since the rate data given in ref 5 suggest that $Cu(oxac)_2^{2-}$ has roughly twice the kinetic activity of Cu(oxac), replacement of an $oxac^{2-}$ by a phen should cause a slight decrease in the CO_2 evolution rate, as was observed, owing to an increase in the amount of enol. The addition of other saturated ligands is also expected to yield inhibition.

Considering the previously published results and those of this work, there is little evidence that the groups likely to lie at the active site of an enzyme are capable of conferring on a metal ion special electronic properties that aid the decarboxylation of oxac. Even if a phenanthroline-like environment were present, any gains from this source are expected to be modest compared to other effects the enzyme environment could exert on the distribution of oxac between active Moxac and inactive $M_2(H_{-1}oxac)^+$. Changes in the relative amounts of these species can have marked effects on the rates.

Decarboxylation rate-concentration profiles for metal ion catalyzed reactions of $oxac^{2-}$ have been determined by Speck[20] in the presence and absence of parsley root decarboxylase. The curves for both sets of reactions tend to exhibit maxima, the positions and heights of which are highly dependent on the nature of the metal ion. In the case of the enzyme the maxima lie at lower metal ion concentrations. Also, Mn(II) was found to be a particularly good enzyme activator in contrast to its low activity in the nonenzymatic reactions. Zn(II) showed the highest nonenzymatic rates.

Qualitative arguments based on the existence of primary (activating) and secondary (inhibiting) metal ion binding modes, both of which follow the Irving-Williams order of stabilities, have been proposed[21,22] to explain the metal ion dependent rate profiles. Results obtained for stability determinations of the mononuclear Moxac[9-11,23,24] and dinuclear $M_2(H_{-1}oxac)^+$ [9,23,24] complexes have confirmed these suggestions, showing that the stability order for both types of complexes is indeed, Cu(II) > Zn(II) > Mn(II) > Mg(II). Regarding the high enzymatic activity of Mn(II), it is significant that the stability differences between the dinuclear complexes have been found to be appreciably greater than those between the mononuclear complexes, i.e., $Mn_2(H_{-1}oxac)^+$ is much less stable relative to $Cu_2(H_{-1}oxac)^+$ than Mn(oxac) is to Cu(oxac). Thus, inhibition by Mn(II) is less apt to occur than by a metal ion such as Cu(II) or Zn(II).

To a good approximation, the shapes and positions of the rate-concentration profiles are determined essentially by the f_{Moxac} term in eq 2. Using the formation constants determined in these laboratories for Mn(II), Cu(II), and Zn(II), values of f_{Moxac} were computed as a function of metal ion concentration assuming the same conditions as employed by Speck.[20] The results are plotted in Figure 7A.

A strong resemblance exists between these curves and the corresponding nonenzymatic rate profiles shown in Figure 1 of ref 20. The difference in the relative heights of the curves in these two figures arises from the influence of the terms k_{-CO_2} and K_{enol} of eq 2. Noteworthy, here is the relatively small proportion of Mn(oxac) shown to be formed, except when fairly high concentrations of Mn^{2+} are attained. Comparing the three different metal ions it is also seen that the more stable is the Moxac complex, the lower is the metal ion concentration at which the maximum is found and the smaller is the proportion of Moxac present at the maximum. Only because of the high value of $k_{-CO_2}^{Cu(oxac)}$ is appreciable activity of Cu(oxac) observed.

Striking resemblances to the enzymatic rate-concentration profiles reported by Speck (Figure 4 of ref 20) are borne by the curves shown plotted in Figure 7B. These values of f_{Moxac} have been calculated by using formation constants for Moxac and $M_2(H_{-1}oxac)^+$ which have been multiplied by factors of 10^2 and 10^4, respectively. Compared to the curves in panel A the maxima are shifted to lower concentrations, roughly corresponding to those actually reported for the enzymatic reactions, and an appreciably greater fraction of Mn(oxac) is formed than is the case with Mn(II) and Zn(II). Thus, all the parsley root enzyme need do to yield many of the major features of the observed rate behavior is to stabilize the metal ion-$oxac^{2-}$ complexes relative to the solution phase.[25]

This model shows that Mn(II) occupies a propitious intermediate position. Cu(II) and Zn(II) exhibit higher values of decarboxylation rate constants, but the benefit gained is more than offset by the large tendency of these ions to form inactive enolate complexes. An ion such as Mg(II), which is on the other end of the scale, does not readily form enolate complexes, but also has a low decarboxylation rate constant. The slight increase in f_{Moxac} that is possible with Mg^{2+} is counteracted by a slow decarboxylation rate. These factors can be balanced in Mn(II) to yield optimum activity. All that is needed to achieve this is an environment which increases the stabilities of the complex.

No unusual interactions need be brought into play in order for an enzyme to stabilize a bound complex. A region of low dielectric constant near the active site would bring about an increase in the formation constants of both the mononuclear and dinuclear complexes, the latter to a greater extent than the former, as assumed in the model.[26] The effect here would be electrostatic in nature. Also, present and likely to be involved would be the usual enzyme-substrate interactions that lead to efficient substrate binding.[28] Thus, the behavior of parsley root decarboxylase is consistent with a more, or less, normal metal ion function superimposed upon a more, or less, normal enzyme function.

Supplementary Material Available: Decarboxylation relaxation (7 pages). Ordering information is available on any current masthead page.

References and Notes

(1) We wish to express our appreciation to the National Science Foundation for its support of this work.
(2) R. Steinberger and F. H. Westheimer, *J. Am. Chem. Soc.*, **73**, 429 (1951).
(3) J. V. Rund and R. A. Plane, *J. Am. Chem. Soc.*, **86**, 367 (1964).
(4) J. V. Rund and K. G. Claus, *J. Am. Chem. Soc.*, **89**, 2256 (1967).
(5) M. Munakata, M. Matsui, M. Tabushi, and T. Shigematsu, *Bull. Chem. Soc. Jpn.*, **43**, 114 (1970).
(6) Y. Yamane, M. Miyazaki, N. Yamaji, and T. Ogashiwa, *Chem. Pharm. Bull.*, **19**, 2342 (1971).
(7) P. R. Bontchev and V. Michaylova, *Proc. Symp. Coord. Chem.*, 1, 405 (1970).
(8) G. W. Kosicki and F. H. Westheimer, *Biochemistry*, **7**, 4303 (1968).
(9) N. V. Raghavan and D. L. Leussing, *J. Am. Chem. Soc.*, **98**, 723 (1976).
(10) E. Gelles and R. W. Hay, *J. Chem. Soc.*, 3673 (1958).
(11) E. Gelles and A. Salama, *J. Chem. Soc.*, 3864, 3869 (1958).
(12) G. Schwarzenbach and H. Flaska, "Complexometric Titrations", 2nd English ed, Nethven and Co. Ltd., London, 1969.
(13) V. S. Sharma and D. L. Leussing, *Talanta*, **18**, 1137 (1971).
(14) Owing to variations in pH it was not feasible to plot the remainder of the data on this type of graph. However, all of the data points for each series of investigations were employed in the numerical analyses. The agreement between observed and calculated rates for the final fit is as good in general as is shown in the figures. All of the data are given in the microfilm version.
(15) V. S. Sharma and D. L. Leussing, *Inorg. Chem.*, **11**, 138, 1955 (1972).
(16) H. Sigel, *J. Inorg. Nucl. Chem.*, **37**, 507 (1975).
(17) H. Sigel, "Metal Ions in Biological Systems", Vol. 2, Marcel Dekker, New York, N.Y., 1974, p 63–125.
(18) There is some correlation between the stability constants of $Cu_2(L)(H_{-1}oxac)$ and $Cu_2(L)_2(H_{-1}oxac)$. A high value chosen for the former will yield a low value for the latter, and vice versa. Regardless of the uncertainties in the absolute values of the formation constants, the calculations show that the mixed ligand dinuclear complexes are relatively unstable with respect to the mononuclear complexes.
(19) Of the metal ions studied in ref 5 only Cu(II) has a sufficiently high affinity for $oxac^{2-}$ that the bis complex is likely to be formed under the conditions described. Inhibition at the higher pH examined indicates the formation of mononuclear enolate complexes. In experiments employing dilute solutions, we have found the pK_a of Cu(oxac) to be around 5.8. $Cu(oxac)_2^{2-}$ is expected to exhibit a value of pK_{1a} slightly lower than this, roughly in agreement with the results given in ref 5. We are not able to account for the slight rate enhancement in CO_2 evolution reported when histidine is added to Cu(II)–$oxac^{2-}$ solutions. Our results show that coordinated histidine has about the same influence on coordinated $oxac^{2-}$ as H_2O. Perhaps, because protonated histidine complexes can be formed, $oxac^{2-}$ is merely distributed over a greater number of species that are able to undergo decarboxylation, Cu(oxac), Cu(his)$oxac^-$, and Cu(Hhis)oxac. This explanation invokes a simple statistical effect as the cause.
(20) H. Speck, *J. Biol. Chem.*, **178**, 315 (1949).
(21) G. Eichhorn, *Adv. Chem. Ser.*, **No. 37**, Chapter 3 (1963).
(22) R. J. P. Williams, *Biol. Rev. Cambridge Philos. Soc.*, **28**, 381 (1953), cited in ref 21.
(23) W. D. Covey and D. L. Leussing, *J. Am. Chem. Soc.*, **96**, 3860 (1974).
(24) M. Emlý, has found the formation constants of Mn(oxac) and $Mn_2(H_{-1}oxac)^+$ to be 36 and 2×10^{-4} M^{-1}, respectively, in aqueous media. K_{enol} is about 1 (unpublished results obtained in these laboratories).
(25) The model predicts that Cu(II) should show more enzymatic activity than is observed. The deactivation could arise from (1) the binding of Cu(II) to a second enzyme site, (2) to an unusually high binding constant of the enzyme toward $Cu_2(H_{-1}oxac)^+$, or (3) to the binding of the 1:1 enolate complex, $Cu(H_{-1}oxac)^-$, which was neglected in the calculations.
(26) Rates of decarboxylation have been found to increase in mixed solvent systems of low dielectric constant, ref 3, 7, 27.
(27) C. S. Tsai, Y. T. Lin, C. Reyes-Zamora, and J. A. Fraser, *Bioinorg. Chem.*, **4**, 1 (1974).
(28) B. Vallee and W. E. C. Wacker, "The Proteins", Vol. V, 2nd ed, H. Neurath, Ed., Academic Press, New York, N.Y., 1970.
(29) L. G. Sillen and A. E. Martell, *Spec. Publ., Chem. Soc.*, **No. 17** (1964), and **25** (1971).

Ligand Effects on the Thermodynamic Stabilization of Copper(III)–Peptide Complexes

Frank P. Bossu, K. L. Chellappa, and Dale W. Margerum*

Contribution from the Department of Chemistry, Purdue University, West Lafayette, Indiana 47907.

Received August 16, 1976

Abstract: Electrode potentials are measured for 40 $Cu^{III,II}$–peptide couples (including peptide amides) in aqueous solution. The potentials are very sensitive to changes in the nature of the ligand and span a range from 1.02 to 0.45 V. The values of E^0 decrease with an increase in the number of deprotonated-peptide groups. Bound hydroxide groups in the place of equatorial carboxylate groups and C-substituents in the chelated amino acid residues also decrease the value of E^0, but to a lesser extent. Histidine-containing peptide complexes have relatively high values of E^0. The additivity of the individual ligand effects allows the electrode potential of a copper complex to be estimated on the basis of the nature of the ligand. The triply deprotonated peptide complexes and the highly C-substituted tripeptide complexes of copper have effective potentials at physiological pH such that O_2 oxidation to Cu(III) is thermodynamically possible. From a correlation between the potentials and visible absorption maxima of the copper(II) peptides it is concluded that the relative gain in the crystal field stabilization energy for the change from d^9 Cu(II) to d^8 Cu(III) is an important factor in the overall thermodynamic stability of the Cu(III)–peptide complexes.

Trivalent copper has generally been considered to be an uncommon oxidation state, although a limited number of Cu(III) compounds have been identified in the solid state[1,2] and a few complexes have been prepared in nonaqueous solutions.[3,4] In aqueous solution Cu(III)–aquo and Cu(III)–amine complexes, generated by pulse radiolysis, are transient species which decay rapidly.[5] In the work of Levitski, Anbar, and Berger,[6] $IrCl_6^{2-}$ was used to oxidize Cu(II)–tetra-L-alanine to a Cu(III) complex which was proposed as an intermediate species prior to further oxidation and fragmentation of the peptide. Bour and Steggerda[2] isolated crystalline Cu(III) complexes of biuret and oxamide, providing some of the first evidence that Cu(III) could be stabilized by deprotonated amide groups. The copper(II) complexes of oligopeptides promote ionization of the peptide hydrogens upon complexation and the resulting deprotonated-peptide groups are strong in-plane donors. Systematic studies of the solution behavior of oligopeptide complexes using potentiometric and spectrophotometric methods have given copper(II)–peptide stability constants and have provided evidence for coordination of the deprotonated-peptide group.[7-15]

The copper complexes of diglycine, triglycine, and tetraglycine were studied by infrared (D_2O solutions) in addition to the other techniques and also gave evidence for deprotonated-peptide nitrogen bonding.[16-18] ESR has been used to study several copper(II)–peptide complexes,[19-21] while ORD-CD has been used to examine nickel(II)–peptide complexes.[22] In addition both divalent nickel and copper complexes have been studied with proton NMR.[23] In a complex with ligands such as tetraglycine as many as three deprotonated-